Mendeleev Communications

Mendeleev Commun., 2027, **37**, in press

Adsorption of CO, C_2H_2, and C_2H_4 on Cu–Pd single-atom alloy catalysts: a DFT investigation

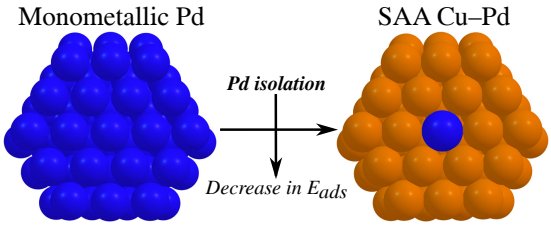
Artyom R. Kolyadenkov,[a] Daria A. Pichugina,[b] Nadezhda S. Smirnova,[a] Igor S. Mashkovsky*[a] and Alexander Yu. Stakheev[a]

[a] *N. D. Zelinsky Institute of Organic Chemistry, Russian Academy of Sciences, 119991 Moscow, Russian Federation. E-mail: kar@ioc.ac.ru*

[b] *Department of Chemistry, M. V. Lomonosov Moscow State University, 119991 Moscow, Russian Federation*

DOI: 10.71267/mencom.8153

Systematic DFT calculations were performed to investigate the adsorption of CO, C_2H_2, and C_2H_4 on model Pd_{64} and $Cu_{63}Pd$ clusters. The transition to a single-atom alloy structure induced a substantial weakening of binding energies for all considered molecules. Both ensemble and electronic effects explained the enhanced ethylene selectivity on Pd–Cu single-atom alloy sites.



Keywords: single-atom alloy catalysts, selective acetylene hydrogenation, density functional theory, copper–palladium catalyst, gas adsorption, synergistic effect.

Selective hydrogenation of acetylene to ethylene is an important industrial process for the removal of alkyne impurities from the ethane–ethylene fraction prior to polymerization.[1–4] Heterogeneous catalysts based on palladium catalyze the process. Under real process-stream conditions (front-end scheme), the reaction mixture always contains trace amounts of CO, which can bind strongly to Pd adsorption sites, acting either as a selective modifier or a catalytic poison.[5–7] Instead of monometallic particles, the application of single-atom alloy (SAA) catalyst structures[8,9] has a great potential. On SAA structures, isolated palladium atoms are stabilized in a matrix of a less active metal, notably copper.[10] In this regard, understanding fundamental principles governing the adsorption of unsaturated hydrocarbons and carbon monoxide on palladium-based SAA catalysts is a key aspect for the rational design of highly selective hydrogenation systems.[1,2] Previous experimental and theoretical studies confirmed that the formation of Pd–Cu single-atom alloys makes it possible to drastically suppress the undesired over-hydrogenation of ethylene to ethane owing to the disruption of extended palladium ensembles.[11–13] The general principles of molecular hydrogen activation on isolated SAA sites with subsequent spillover onto the copper support have been described in detail,[14–16] and the isolated chemisorption of C_2H_2 and C_2H_4 molecules on flat facets has also been investigated.[17–19] However, systematic quantum-chemical studies devoted to the nature of changes in the binding of CO, acetylene, and ethylene upon a transition from monometallic Pd phases to isolated palladium sites are comparatively small in number.[19] A comprehensive understanding of this factor at the atomic level is necessary to control catalyst selectivity in the selective hydrogenation of acetylene.

Thus, the aim of this work was a density functional theory (DFT) study of the adsorption of C_2H_2, C_2H_4, and CO on model Pd_{64} and $Cu_{63}Pd$ clusters, which simulated a monometallic palladium surface and a bimetallic PdCu single-atom alloy catalyst, respectively. The main focus was on elucidating the specific adsorption properties of Pd sites isolated in a copper matrix. A similar approach was used to simulate the adsorption and catalytic properties of catalysts based on transition metal particles.[20]

Details of quantum chemical calculations for the clusters, adsorbate molecules, and adsorption complexes are described in the Online Supplementary Materials. The adsorption energies E_{ads}(G/C) of adsorbate G (C_2H_2, C_2H_4 or CO) on cluster C (Pd_{64} or $Cu_{63}Pd$) were calculated according to the formula

$$E_{ads}(G/C) = [E(G) + ZPVE(G)] + [E(C) + ZPVE(C)] - [E(G/C) + ZPVE(G/C)],$$

where E and $ZPVE$ are the absolute energy and the zero-point vibrational energy correction of free adsorbates (G), clusters (C), and adsorption complexes (G/C), respectively.

The Pd_{64} cluster was constructed as a three-layer fragment of the palladium lattice with a (111) top facet [Figure 1(*a*)]. The $Cu_{63}Pd$ cluster was built in two steps: first, a Cu_{64} cluster was cut from the copper lattice in the same manner and fully optimized; then, one surface Cu atom was replaced by Pd, and the resulting structure was re-optimized Figure 1(*b*). Both Pd_{64} and $Cu_{63}Pd$ clusters are thermodynamically stable with binding energies of 3.28 and 2.78 eV per atom, respectively. The models were validated against experimental EXAFS data. The average calculated Pd–Pd distance in Pd_{64} (2.72 Å) and Pd–Cu distance

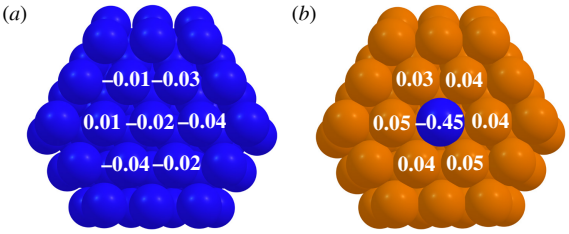


Figure 1 General view of the (*a*) Pd_{64} and (*b*) $Cu_{63}Pd$ clusters along with the Bader charges for selected atoms therein. Pd and Cu atoms are colored blue and orange, respectively.

© 2027 Mendeleev Communications

in $Cu_{63}Pd$ (2.57 Å) agreed well with experimental values reported for $Pd_{0.006}/SiO_2$ (2.73 Å) and $CuPd_{0.006}/SiO_2$ (2.58 Å) catalysts.[11] Thus, the chosen cluster model adequately represented the local environment of an active metal site.

An analysis of the electronic structures revealed fundamental differences in the state of palladium upon its transition from its own phase into a copper matrix. Bader charge calculations showed that a transfer of electron density in the bimetallic $Cu_{63}Pd$ cluster occurred from the copper atoms to the palladium atom (Figure 1). A consequence of this charge redistribution was a modification of the density of electronic states. The observed shift of the Pd *d*-states downward on the energy scale relative to the highest occupied molecular orbital (HOMO) level (Figure 2) indicated their filling, which was an important factor governing the chemisorption properties of an isolated site.

According to simulation data, CO, C_2H_2, and C_2H_4 had multi-site coordination during the adsorption on the monometallic Pd_{64}. In particular, carbon monoxide adsorbed at three-fold sites with the C–O bond elongated to 1.19 Å; acetylene had the classic adsorbed μ-form coordinated to three palladium atoms with the C–C bond stretched to 1.38 Å, and ethylene formed a di-σ-bonded complex with two palladium atoms, where the C–C distance increased to 1.47 Å [Figures 3(*a*)–(*c*)]. Compared to the bond lengths in the free molecules (1.14 Å for CO, 1.21 Å for C_2H_2, and 1.33 Å for C_2H_4), these elongations indicated significant activation of the adsorbed species. These results fully correlated with the adsorption of these molecules on the Pd(111) surface calculated previously.[21] The adsorption energies are collected in Figure 4(*a*). The adsorption energies were high for CO (1.80 eV) and C_2H_2 (1.78 eV), whereas C_2H_4 was bound noticeably more weakly (0.82 eV).

During the adsorption on the bimetallic $Cu_{63}Pd$ cluster, a reorganization of the adsorption complexes geometry was observed due to changes in the surface structures [Figures 3(*d*)–(*f*)]. The palladium atom isolated in a copper environment became the binding site for carbon monoxide and ethylene, whose adsorption acquired a one-centre (linear for CO) character. For CO, the C–O bond length was 1.16 Å, slightly elongated compared to 1.14 Å in the free molecule. The most remarkable changes were observed upon acetylene adsorption. Instead of the expected binding to the Pd atom only, a transition to four-centre coordination occurred: the C_2H_2 molecule simultaneously interacted with the single palladium atom and three neighboring copper atoms to form a $PdCu_3$-type site. In this complex, the C–C bond was stretched to 1.38 Å (free, 1.21 Å). Ethylene adsorbed *via* the Pd atom with the C–C bond length of 1.38 Å (free, 1.33 Å). Note that an analogous structure of the adsorption complex was previously predicted theoretically.[22] These structural transformations were accompanied by a considerable decrease in the energy for all three molecules

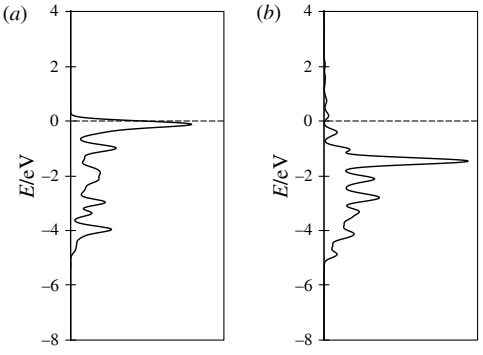


Figure 2 Partial densities of *d*-states (d-PDOS) for the Pd atoms in the (*a*) Pd_{64} and (*b*) $Cu_{63}Pd$ clusters. The dashed lines denote the HOMO levels of the clusters.

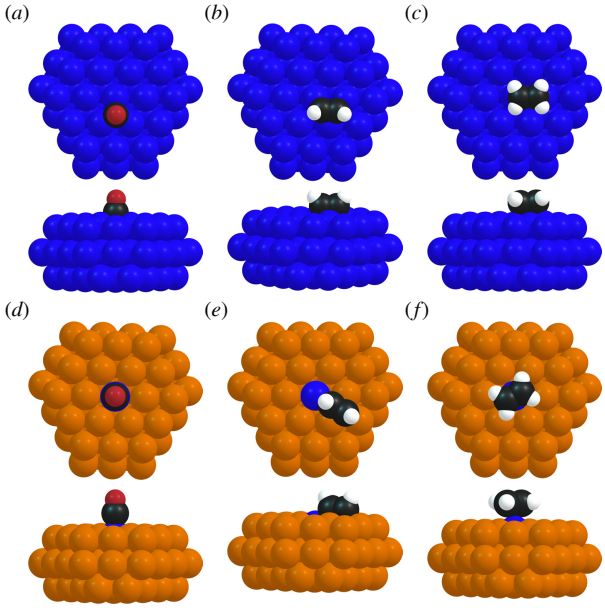


Figure 3 Geometric structures of the adsorption complexes (*a*)CO/Pd_{64}, (*b*) C_2H_2/Pd_{64}, (*c*) C_2H_4/Pd_{64}, (*d*) $CO/Cu_{63}Pd$, (*e*) $C_2H_2/Cu_{63}Pd$, and (*f*) $C_2H_4/Cu_{63}Pd$. Top and side views are shown; H, C, and O atoms are colored white, black, and red, respectively.

compared to Pd_{64} [Figure 4(*b*)]. Thus, the adsorption energies of CO, C_2H_2, and C_2H_4 decreased to 1.11, 1.04, and 0.66 eV, respectively. Ethylene had the lowest surface interaction energy, as was also the case in the palladium cluster. Interestingly, on the SAA surface, the parity of CO and C_2H_2 adsorption energies observed on pure Pd was broken: the CO binding energy now somewhat exceeded that of acetylene (the difference was 0.07 eV). Detailed structural parameters are provided in the Supplementary Materials.

The pronounced weakening of adsorption upon the transition from Pd_{64} to $Cu_{63}Pd$ resulted from the combined action of geometric and electronic factors. The geometric, or ensemble, effect manifested itself in the disruption of contiguous palladium sites and the formation of isolated single-atom active positions. This directly altered the coordination mode: a transition from multi-centre to one-centre adsorption for CO and C_2H_4, which naturally reduced the total binding energy. The situation with acetylene was more complex but still fitted this logic. Despite the increase in the number of atoms directly contacting the molecule (from three to four), three of the four bonds were formed by Cu atoms, which interacted with the adsorbate weaker than Pd. The replacement of three strong Pd–C interactions by weak Cu–C interactions led to a net decrease in the adsorption energy even with a formal increase in the coordination number. The electronic factor, in turn, was caused by the charge redistribution described above. The appearance of the excess electron density on the Pd atom and the concomitant downshift of its *d*-band away from the Fermi level weakened the covalent component of the bond with the adsorbate, which manifested itself as an overall decrease in

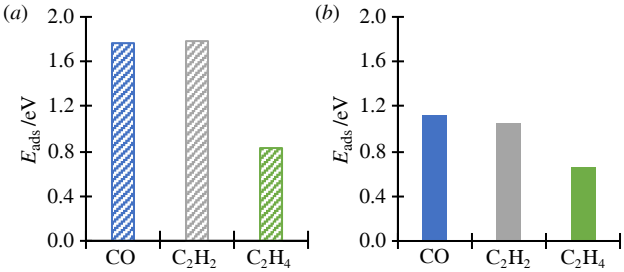


Figure 4 Adsorption energies (E_{ads}) of CO, C_2H_2, and C_2H_4 on the clusters (*a*) Pd_{64} and (*b*) $Cu_{63}Pd$.

the adsorption ability of both the Pd atom itself and the sites involving it.

Thus, the DFT study demonstrated that a transition from the monometallic Pd system to the bimetallic $Cu_{63}Pd$ SAA structure led to a fundamental weakening of the adsorption of acetylene, ethylene, and carbon monoxide. Specifically, the adsorption energies decreased from 1.80 to 1.11 eV for CO, from 1.78 to 1.04 eV for C_2H_2, and from 0.82 to 0.66 eV for C_2H_4. At the same time, the lowest adsorption energy was observed for ethylene on both the bimetallic and monometallic sites. The theoretical results correlated well with the experimentally observed increase in ethylene selectivity in the selective hydrogenation of acetylene upon switching from monometallic palladium catalysts to PdCu SAA compositions. The weaker adsorption of the target product facilitated its desorption from the surface to prevent further hydrogenation to ethane and increase the reaction yield. The key reason for the observed changes was a synergistic combination of electronic and geometric effects induced by the embedding of isolated palladium atoms into a copper matrix. This was manifested in the modification of the Pd *d*-states and the altered binding mode of the molecules.

This work was supported by the Russian Science Foundation (grant no. 23-13-00301-P).

Online Supplementary Materials

Supplementary data associated with this article can be found in the online version at doi: 10.71267/mencom.8153.

References

1 X. Lan, J. G. Chen and T. Wang, *Chem. Soc. Rev.*, 2025, **54**, 7654; https://doi.org/10.1039/d4cs01237b.
2 Yu. V. Gyrdymova and K. S. Rodygin, *Russ. Chem. Rev.*, 2025, **94**, RCR5182; https://doi.org/10.59761/RCR5182.
3 P. V. Markov, I. S. Mashkovsky, G. N. Baeva, D. P. Melnikov and A. Yu. Stakheev, *Mendeleev Commun.*, 2023, **33**, 836; https://doi.org/10.1016/j.mencom.2023.10.032.
4 I. S. Mashkovsky, N. S. Smirnova, P. V. Markov, G. N. Baeva, A. E. Vaulina, D. P. Melnikov and A. Yu. Stakheev, *Mendeleev Commun.*, 2024, **34**, 718; https://doi.org/10.1016/j.mencom.2024.09.030.
5 A. Borodzinski and G. C. Bond, *Catal. Rev.*, 2007, **48**, 91; https://doi.org/10.1080/01614940500364909.
6 M. Jørgensen and H. Grönbeck, *J. Am. Chem. Soc.,* 2019, **141**, 8541; https://doi.org/10.1021/jacs.9b02132.
7 P. V. Markov, N. S. Smirnova, G. N. Baeva, I. S. Mashkovsky, A. V. Bukhtiyarov, I. A. Chetyrin, Ya. V. Zubavichus and A. Yu. Stakheev, *Mendeleev Commun.*, 2023, **33**, 812; https://doi.org/10.1016/j.mencom.2023.10.024.
8 I. S. Mashkovsky, P. V. Markov, A. V. Rassolov, E. D. Patil and A. Yu. Stakheev, *Russ. Chem. Rev.*, 2023, **92**, RCR5087; https://doi.org/10.59761/RCR5087.
9 R. T. Hannagan, G. Giannakakis, M. Flytzani-Stephanopoulos and E. C. H. Sykes, *Chem. Rev.*, 2020, **120**, 12044; https://doi.org/10.1021/acs.chemrev.0c00078.
10 G. Kyriakou, M. B. Boucher, A. D. Jewell, E. A. Lewis, T. J. Lawton, A. E. Baber, H. L. Tierney, M. Flytzani-Stephanopoulos and E. C. H. Sykes, *Science*, 2012, **335**, 1209; https://doi.org/10.1126/science.1215864.
11 G. X. Pei, X. Y. Liu, A. Wang, A. F. Lee, M. A. Isaacs, L. Li, X. Pan, X. Yang, K. Wilson, L. Cui and T. Zhang, *ACS Catal.*, 2017, **7**, 1491; https://doi.org/10.1021/acscatal.6b03293.
12 I. S. Mashkovsky, P. V. Markov, G. N. Baeva, A. E. Vaulina, N. S. Smirnova, D. P. Melnikov and A. Yu. Stakheev, *Mendeleev Commun.*, 2025, **35**, 711; https://doi.org/10.71267/mencom.7850.
13 Y. Ma, Y. Jiang, P. Liu, Y. Jiang and J. Hu, *Appl. Surf. Sci.*, 2017, **410**, 374; https://doi.org/10.1016/j.apsusc.2017.03.122.
14 W. Osada, S. Tanaka, K. Mukai, M. Kawamura, Y. Choi, F. Ozaki, T. Ozaki and J. Yoshinobu, *Phys. Chem. Chem. Phys.*, 2022, **24**, 21705; https://doi.org/10.1039/D2CP01652D.
15 H. L. Tierney, A. E. Baber, J. R. Kitchin and E. C. H. Sykes, *Phys. Rev. Lett.*, 2009, **103**, 246102; https://doi.org/10.1103/PhysRevLett.103.246102.
16 J. Greeley and M. Mavrikakis, *J. Phys. Chem. B*, 2005, **109**, 3460; https://doi.org/10.1021/jp046540q.
17 Y. Huang and Z.-X. Chen, *Appl. Surf. Sci.*, 2022, **575**, 151513; https://doi.org/10.1016/j.apsusc.2021.151513.
18 Y. Qi, B. Wang, M. Fan, D. Li and R. Zhang, *Chem. Eng. Sci.*, 2021, **243**, 116786; https://doi.org/10.1016/j.ces.2021.116786.
19 D. Yuan, Y. Ding, X. Sun and J. Huang, *Phys. Chem. Chem. Phys.*, 2021, **23**, 9025; https://doi.org/10.1039/D0CP05285J.
20 S. S. Laletina, M. Mamatkulov, A. M. Shor, E. A. Shor, V. V. Kaichev and I. V. Yudanov, *Nanoscale*, 2022, **14**, 11; https://doi.org/10.1039/d1nr07947f.
21 N. López, B. Bridier and J. Pérez-Ramírez, *J. Phys. Chem. C*, 2008, **112**, 9346; https://doi.org/10.1021/jp711258q.
22 K. Yang and B. Yang, *Phys. Chem. Chem. Phys.*, 2017, **19**, 18010; https://doi.org/10.1039/C7CP02152F.

Received: 21st July 2026; Com. 26/8153

Contents entry

Adsorption of CO, C_2H_2, and C_2H_4 on Cu–Pd single-atom alloy catalysts: a DFT investigation

Artyom R. Kolyadenkov, Daria A. Pichugina, Nadezhda S. Smirnova, Igor S. Mashkovsky, Alexander Yu. Stakheev

